

Synthesis and discovery of a novel pyrazole derivative as an inhibitor of apoptosis through modulating integrin $\beta 4$, ROS, and p53 levels in vascular endothelial cells

Bao-Xiang Zhao,^{a,*} Lu Zhang,^{b,c} Xing-Shang Zhu,^{b,c} Mao-Sheng Wan,^d Jing Zhao,^{b,c} Yun Zhang,^c Shang-Li Zhang^{b,c} and Jun-Ying Miao^{b,c,*}

^a*Institute of Organic Chemistry, School of Chemistry and Chemical Engineering, Shandong University, Jinan 250100, China*

^b*Institute of Developmental Biology, School of Life Science, Shandong University, Jinan 250100, China*

^c*The Key Laboratory of Cardiovascular Remodeling and Function Research, Chinese Ministry of Education and Chinese Ministry of Health, Shandong University Qilu Hospital, Jinan 250100, China*

^d*Shandong Drug and Food Vocational College, Weihai 264210, China*

Received 30 January 2008; revised 2 March 2008; accepted 4 March 2008

Available online 6 March 2008

Abstract—Recently, pyrazole derivatives as high affinity and selective A2A adenosine receptor antagonists have been reported. But, so far, there are no reports about the inhibitory effects of multi-substituted pyrazole derivatives on apoptosis of vascular endothelial cells (VECs). In this study, we synthesized six pyrazole derivatives and characterized the structures of the compounds by IR, ¹H NMR, mass spectroscopy, and element analysis. The biology assay showed that a novel pyrazole derivative, ethyl 3-(*o*-chlorophenyl)-5-methyl-1-phenyl-1*H*-pyrazole-4-carboxylate (MPD) at low concentration (25 μ M) increased VECs viability and inhibited VECs apoptosis induced by deprivation of serum and FGF-2. During this process, the levels of integrin $\beta 4$, reactive oxygen species (ROS), and p53 were depressed obviously. The data suggested that MPD was a potential inhibitor of apoptosis associated with the signal pathway mediated by integrin $\beta 4$, ROS, and p53 in VECs.

© 2008 Elsevier Ltd. All rights reserved.

1. Introduction

Vascular endothelial cells (VEC) form the inner lining of all blood vessels and function to maintain vascular tone and anticoagulant properties of blood vessels. VEC apoptosis is important in many disease states, including atherosclerosis. Traditional hypotheses of atherogenesis have suggested that the injury of VECs is critical for the development of atherosclerosis.¹ The sites where plaques develop may be associated with increased VEC turnover rate, suggesting a mechanical link with susceptibility to atherosclerosis, perhaps as an increase in apoptosis.² In addition, membrane vesicles from apoptotic cells contain biologically active oxidized phospholipids that can induce monocyte adhesion to the endothelium.^{3,4} In this

way, the inflammatory infiltrate within lesions perpetuates and amplifies the increased apoptosis within lesions. Apoptosis of VECs leads to increased risk for thrombosis. During apoptosis VECs lose anticoagulant membrane components and become procoagulant by an increased exposure of phosphatidylserine on their surface. In the presence of coagulation factors V and VII, phosphatidylserine can promote thrombin generation.⁵ It is presumed that the inhibition of VEC apoptosis can be a clue to the development of new strategies in atherosclerosis therapy.

The use of small molecules to affect biological phenomena, also known as chemical genetics, has made a significant impact in diverse areas of biology.^{6–8} The design of the library is the first and a very crucial step in the forward chemical genetics process, and this step determines the success of the library.⁹ In addition to natural products library and known drug-like library, the design and synthesis of novel small molecules library with valuable chemical diversity has been shown to be challenging.¹⁰

Keywords: Pyrazole derivative; Apoptosis; Vascular endothelial cell; Integrin $\beta 4$; ROS; p53.

* Corresponding authors. Tel.: +86 531 88366425; fax: +86 531 88564464; e-mail addresses: bxzhao@sdu.edu.cn; miaojy@sdu.edu.cn

The pyrazole unit is one of the core structures in a number of natural products. Many pyrazole derivatives are known to exhibit a wide range of biological properties and have been attracted attention in the widely field of biology. Extensive studies have been devoted to arylpyrazole derivatives such as Celecoxib, a well-known cyclooxygenase-2 inhibitor.^{11–14} Recently, pyrazole derivatives as high affinity and selective A2B adenosine receptor antagonists have been reported.¹⁵ But, so far, there are no reports about the effects of pyrazole derivatives, especially multi-substituted pyrazole derivatives, on the apoptosis of vascular endothelial cells. In our previous papers, we described the synthesis and preliminary biological evaluation of novel 1-substituted-3-aryl-1*H*-pyrazole-5-carboxylate derivatives and novel 5-alkyl-2-ferrocenyl-6,7-dihydropyrazolo[1,5-*a*]pyrazin-4(5*H*)-one derivatives.^{16–19} In an ongoing study in our laboratory on the discovery and the development of apoptosis inducers or inhibitor as potential new atherosclerosis therapy,^{20–22} we are interested in synthesizing novel multi-substituted pyrazole derivatives and screening potential small molecules for the investigation of molecular mechanism.

Herein, we would like to report the synthesis of novel multi-substituted pyrazole derivatives and the findings of their biological activities in VEC apoptosis, especially, the modulation of ethyl 3-(*o*-chlorophenyl)-5-methyl-1-phenyl-1*H*-pyrazole-4-carboxylate (MPD) on the levels of integrin β 4, reactive oxygen species (ROS), and p53 which play important roles in VECs apoptotic signaling.

2. Results and discussion

2.1. Chemistry

Multi-substituted pyrazole derivatives **4** were synthesized as outlined in Figure 1. The precursors **3** to the multi-substituted pyrazole derivatives were easily synthesized by the treatment of ethyl acetoacetate with the appropriate aryl acid chlorides in the mixture of aqueous solution of sodium hydroxide and petroleum ether. The desired pyrazole derivatives **4** were obtained by the reaction of **3** with hydrazine hydrate and phenyl hydrazine in ethanol at refluxing condition. The struc-

tures of compounds **4** were characterized by IR, ¹H NMR, mass spectroscopy, and element analysis.

Interestingly, when **3a–3c** were treated with hydrazine hydrate, respectively, and **3a** was treated with phenyl hydrazine in ethanol, **4a–4d** were obtained in good yields; however, the reaction of **3b** with phenyl hydrazine and the reaction of **3d** with hydrazine hydrate gave **4e** and **4f**. The structures of compounds **4a–4f** were assigned with ¹H NMR, IR, and mass spectrum. Furthermore, intermediates **3'** and **3** exist in tautomerism. It was reported that the melting point of intermediate **3c'** was 55–56 °C,²³ however, in the present study, we observed that the melting point of **3c** was 128–131 °C. It is not surprising there is the difference because intermediates **3'** and **3** exist in tautomerism and can be isolated in suitable condition.

2.2. Effects of the compounds **4** on VEC apoptosis

In order to evaluate the effects of the compounds on VEC apoptosis, we used the given model of VEC apoptosis induced by deprivation of serum and FGF-2. The 3-(4,5-dimethylthiazol-2-yl)-2,5-diphenyl-tetrazolium bromide (MTT) cell proliferation assay is widely accepted as a reliable way to measure the cell proliferation rate, and conversely when metabolic events lead to apoptosis or necrosis. The results showed that compounds **4a**, **4b**, **4e**, and **4f** had no obvious effects on VEC apoptosis at the concentrations of 25–100 μ M (data not shown), meanwhile it was interesting that ethyl 3-(*o*-chlorophenyl)-5-methyl-1-phenyl-1*H*-pyrazole-4-carboxylate **4d** (MPD) suppressed the apoptosis at 25 μ M and promoted the apoptosis at the concentrations of 50 and 100 μ M ($p < 0.01$) (Fig. 2). This finding is similar to the phenomena observed in our previous study with other small molecules.^{20,24}

2.3. Effects of compound MPD on the morphological changes of VECs

When VECs were deprived of FGF-2 and serum, cell growth was inhibited ($p < 0.01$), and the cells gradually detached from the dish and apoptosis occurred (Fig. 2B and E). After treatment with MPD from 5 to 100 μ M for 24 and 48 h, we examined the changes of morphology and viability of the cells. The results

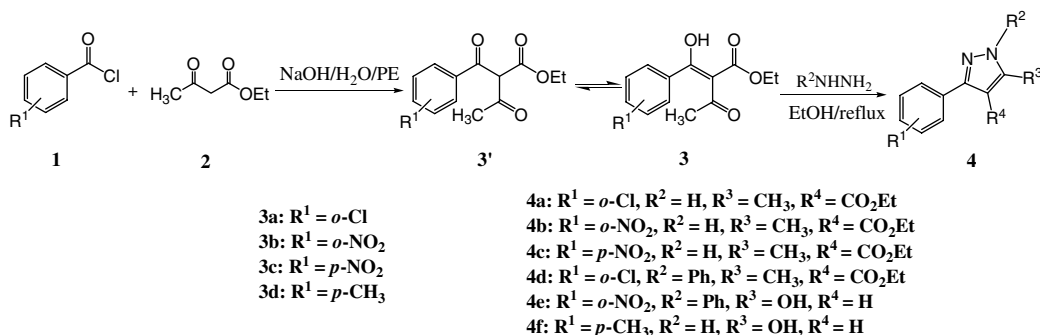


Figure 1. Scheme for the synthesis of multi-substituted pyrazole derivatives.

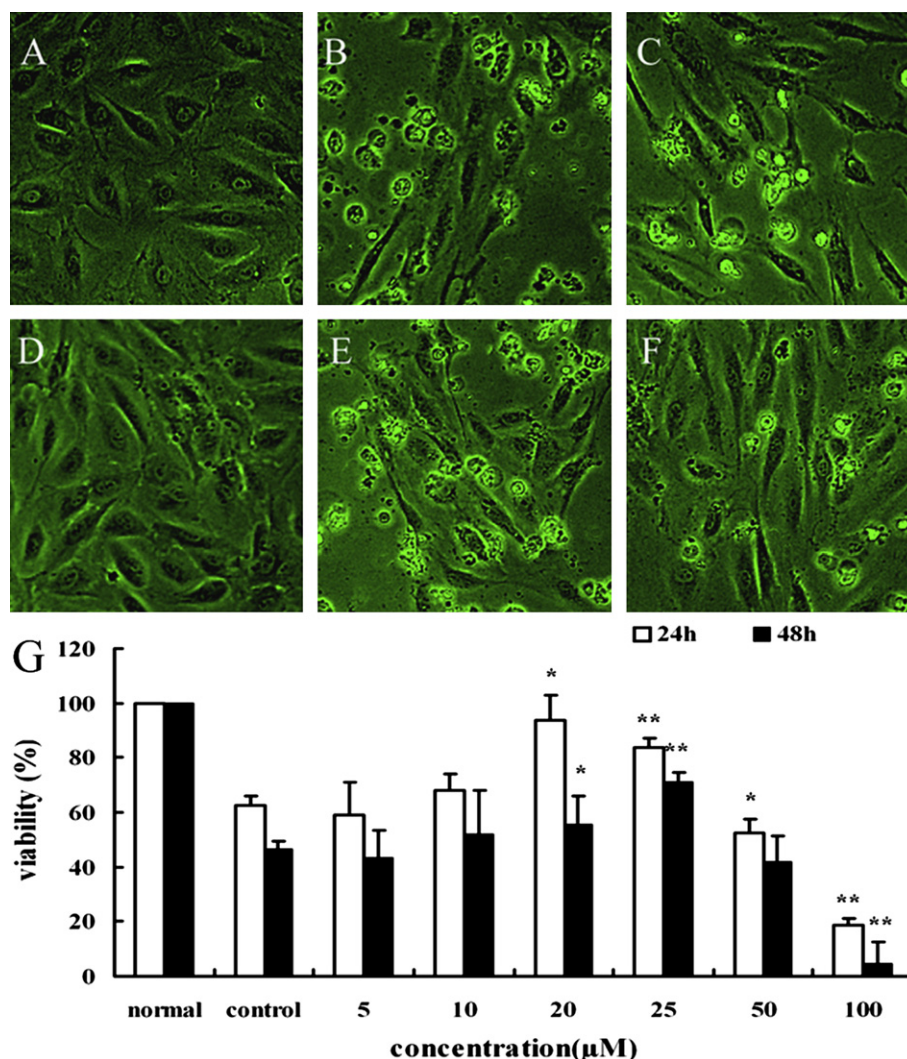


Figure 2. Effects of MPD on cell morphology and viability of VECs. (A and D) Cells cultured in M199 medium with serum and FGF-2 for 24 and 48 h, respectively. (B and E) Cells cultured in basal M199 for 24 and 48 h, respectively. (C and F) Cells treated with MPD at 25 μM for 24 and 48 h, respectively. (G) Effects of MPD on viability of VECs. Normal, cells cultured in M199 medium with serum and FGF-2. Control, cells cultured in basal M199 medium (without serum and FGF-2). 5, 10, 20, 25, 50 and 100, cells treated with MPD at 5, 10, 20, 25, 50 and 100 μM, respectively. (* $p < 0.05$, ** $p < 0.01$ vs control group, $n = 3$).

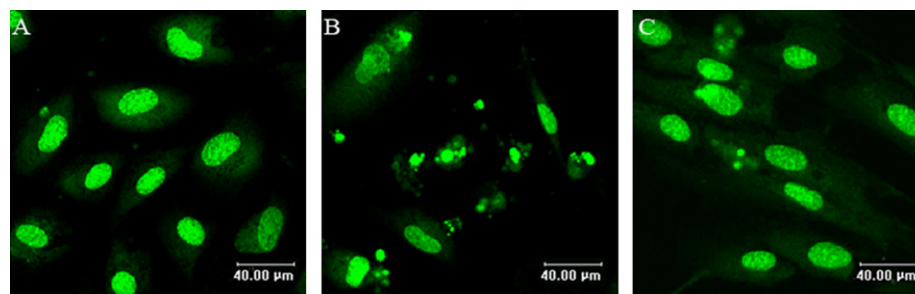


Figure 3. Effects of MPD on nuclear DNA fragmentation. (A) Nuclei of normal cells cultured in M199 medium with serum and FGF-2. (B) Nuclei of control cells deprived of serum and FGF-2 for 24 h. (C) Nuclei of cells treated with MPD at 25 μM for 24 h.

showed that MPD most effectively increased the cell viability at 25 μM. The morphological changes associated with apoptosis were impaired compared with the control (Fig. 2C, F, and G). Thus, 25 μM concentration of MPD was used in the next experiments.

2.4. Effects of the compound MPD on nuclear DNA condensation and fragmentation in VECs

In order to confirm the anti-apoptotic effect of the compound MPD, its effects on nuclear DNA condensation

and fragmentation in VECs were analyzed by acridine orange (AO) staining and TUNEL assay. The results showed that nuclear DNA condensation and fragmentation were inhibited obviously when the cells were exposed to MPD at 25 μM for 24 h (Fig. 3). When the cells were deprived of serum and FGF-2 for 24 h, the proportion of apoptotic cells was $41.38 \pm 3.74\%$, which was much higher than that in the normal group ($p < 0.01$) (Fig. 4A, B, and D). After VECs were treated with MPD at 25 μM for 24 h, the proportion of apoptotic cells was reduced to $19.16 \pm 5.53\%$ ($p < 0.01$) (Fig. 4C and D). The result showed that MPD could effectively inhibit VEC apoptosis induced by deprivation of serum and FGF-2.

Taken together, these findings encouraged us to investigate the mechanism of MPD action and its modulation on the levels of integrin $\beta 4$, ROS, and p53 which play important roles in VEC apoptotic signaling.^{25–27}

2.5. The compound MPD depressed the level of integrin $\beta 4$

Integrin $\beta 4$ is found in hemidesmosomes, providing firm mechanical links between the basal lamina and the intermediate filament cytoskeleton system.²⁸ It is a key membrane protein in cellular signal transduction and involved in apoptotic cell death of VECs.^{26,27} Thus, we further explored the effects of MPD on integrin $\beta 4$ level to understand the mechanism of MPD action. In our previous studies, it has been shown that integrin $\beta 4$ is a key factor involved VEC apoptotic signaling.²⁹ In order to know whether MPD can modulate this integrin subunit, we determined the changes of integrin $\beta 4$ level

in MPD-treated VECs. The immunofluorescence results showed that the relative level of integrin $\beta 4$ in the cells deprived of serum and FGF-2 was much higher than that in the normal cells ($^{##}p < 0.05$) (Fig. 5A, B, D, E, G, H, and J). The fluorescent intensity of the cells treated with MPD for 12, 24, and 48 h was 6.307 ± 1.225 , 9.083 ± 1.010 , 13.14 ± 1.667 , respectively. The fluorescent intensity of control group cells (12, 24 and 48 h) was 11.384 ± 1.962 , 11.725 ± 1.404 , 16.331 ± 0.858 , respectively. In the cells treated with MPD for 12 and 48 h, the relative level of integrin $\beta 4$ was depressed obviously ($^*p < 0.05$) (Fig. 5C, I, and J).

2.6. The compound MPD depressed the level of intracellular ROS

It was shown that integrin $\beta 4$ participated in regulation of ROS level in VECs.^{30,31} Therefore, we checked the effects of MPD on ROS level in VECs. In the cells of control group, the relative fluorescent intensity of 2',7'-dichlorofluorescein (DCF) was much higher than that in the normal cells ($p < 0.01$) (Fig. 6A, B, D, E, G, H, and J). But when the cells deprived of serum and FGF-2 were treated with MPD at 25 μM , the fluorescent intensity decreased significantly ($^{**}p < 0.01$ and $^*p < 0.05$) (Fig. 6C, F, I, and J). Our results showed that MPD could depress intracellular ROS levels induced by deprivation of serum and FGF-2.

2.7. The compound MPD depressed the level of p53

Integrin $\beta 4$, ROS, and p53 were involved in the signal pathway of VEC apoptosis induced by deprivation of serum and FGF-2. The levels of p53 protein in the cells

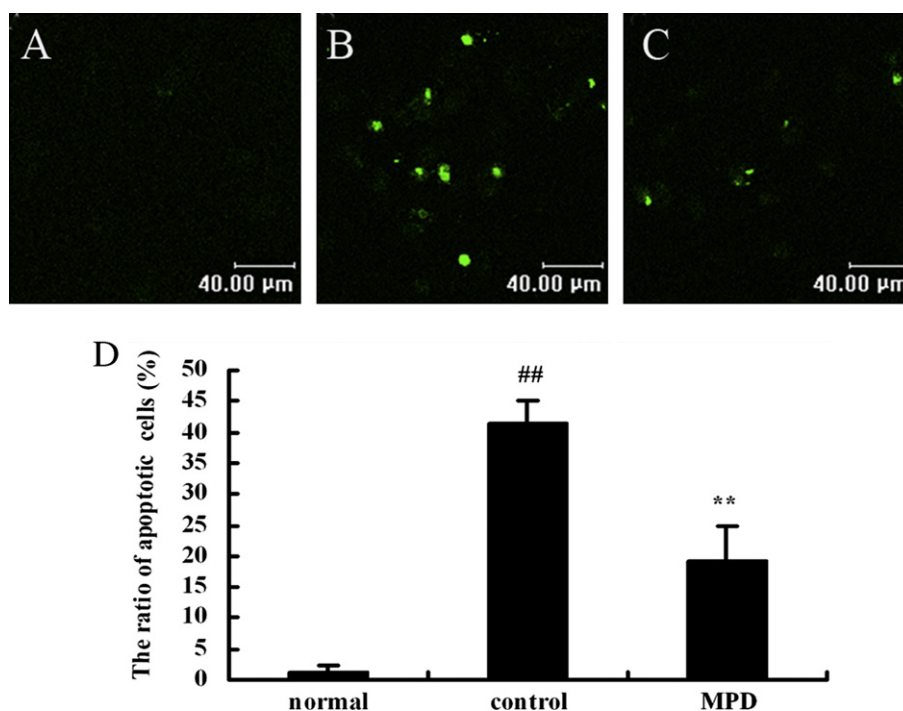


Figure 4. Quantification of apoptotic cells by TUNEL assay. Fluorescent micrographs show the TUNEL staining of VECs. (A) Normal, cells cultured in M199 medium with serum and FGF-2 for 24 h. (B) Control, cells cultured in basal M199 medium for 24 h. (C) Cells treated with MPD at 25 μM for 24 h. (D) The quantity of apoptotic cells ($^{##}p < 0.01$ vs normal group, $^{**}p < 0.01$ vs control group, $n = 3$).

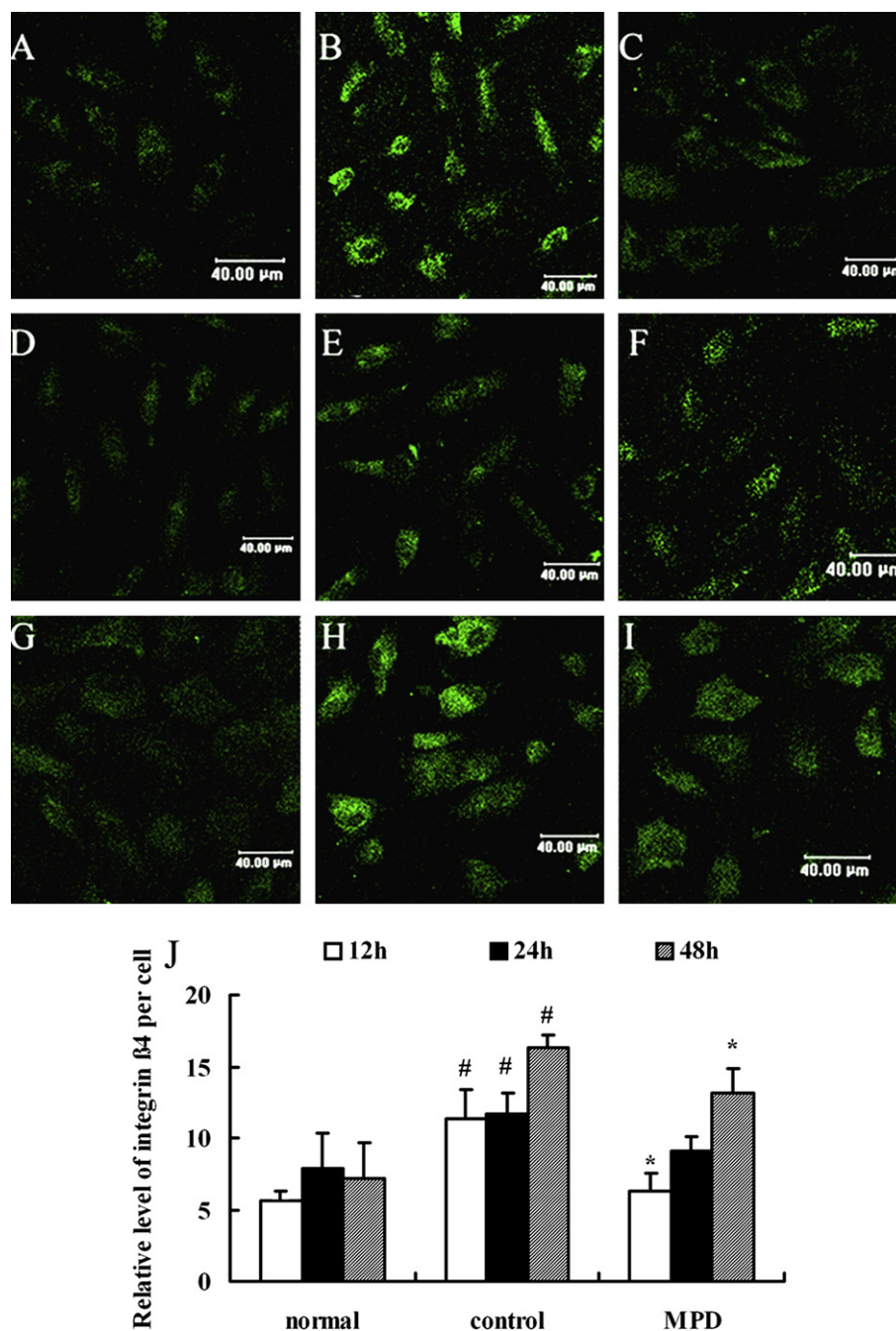


Figure 5. Effects of MPD on the level of integrin $\beta 4$ in VECs. (A–I) Fluorescent micrographs show the relative intensity of integrin $\beta 4$. (A, D and G) Normal, cells cultured in M199 medium with serum and FGF-2 for 12, 24 and 48 h, respectively. (B, E and H) Control, cells deprived of serum and FGF-2 for 12, 24 and 48 h, respectively. (C, F and I) Cells treated with MPD at 25 μM for 12, 24 and 48 h, respectively. (J) The relative quantity of integrin $\beta 4$ level in VECs (# $p < 0.05$ vs normal group, * $p < 0.05$ vs control group, $n = 3$).

deprived of serum and FGF-2 were much higher than that in the normal cells ($p < 0.01$) (Fig. 7A, B, D, E, G, H, and J). But in the MPD-treated cells, the levels of p53 were depressed significantly ($p < 0.01$) (Fig. 7C, F, I, and J). This result showed that the increase of p53 level induced by deprivation of serum and FGF-2 could be inhibited by MPD.

VEC apoptosis is an important mechanism of vascular injury, resulting in vascular leak, inflammation, coagulation and atherosclerotic lesion formation. Therefore,

inhibition of endothelial cell apoptosis is of great importance in various vascular diseases. In the previous researches, we found several kinds of chemical compounds that can promote or inhibit VEC apoptosis. These small molecules are very helpful tools for understanding the mechanisms of VEC apoptosis.^{20,32} Furthermore, they could modulate the level of integrin $\beta 4$ that is a very important integrin subunit in cellular signaling. Our recent report showed that 3-benzyl-5-((2-nitrophenoxy)methyl)-dihydrofuran-2(3H)-one (3BDO) could inhibit VEC apoptosis and suppress integrin $\beta 4$

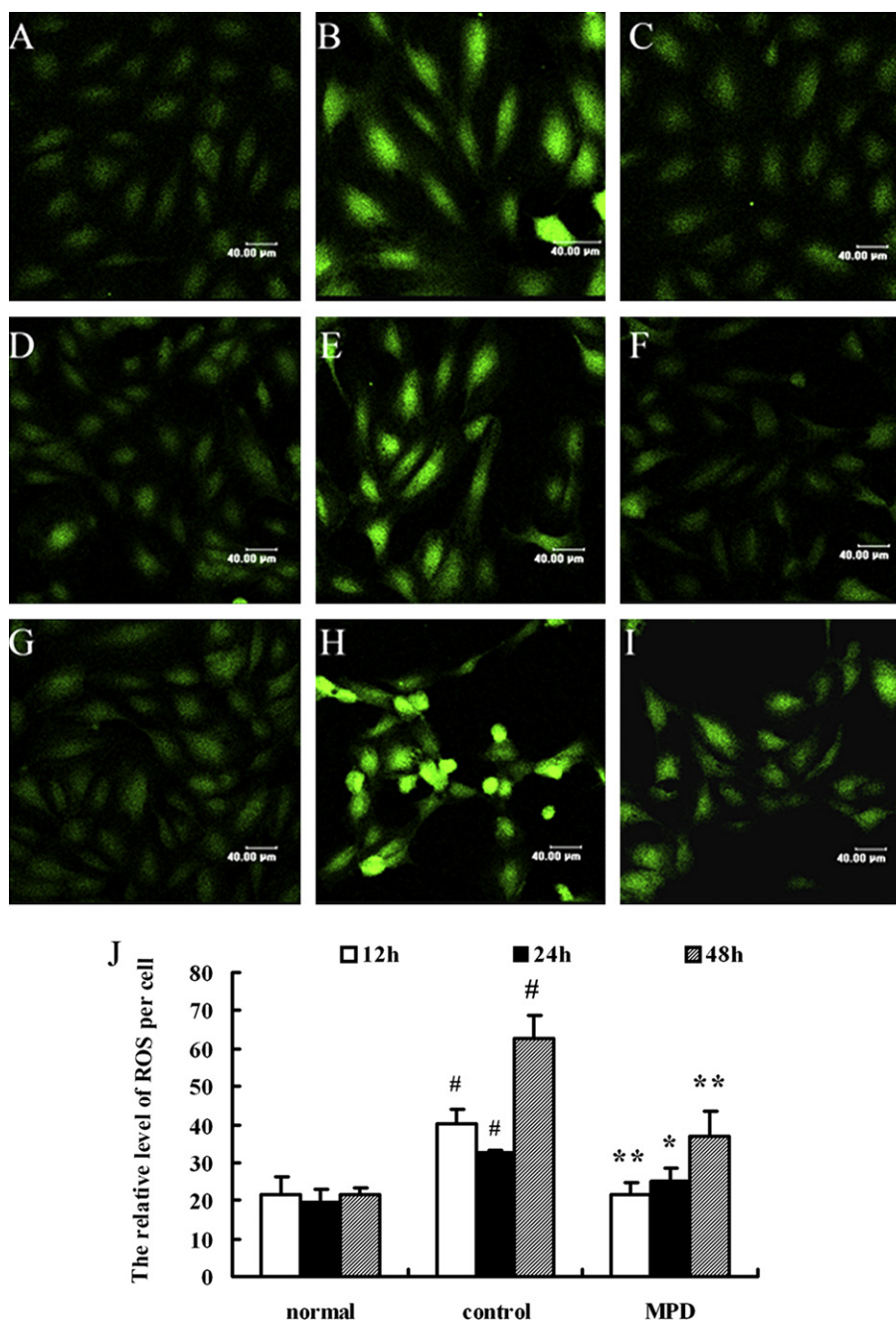


Figure 6. Effects of MPD on the level of ROS in VECs. (A–I) Fluorescent micrographs show the relative intensity of ROS. (A, D and G) Normal, cells cultured in M199 medium with serum and FGF-2 for 12, 24 and 48 h, respectively. (B, E and H) Control, cells deprived of serum and FGF-2. (C, F and I) Cells treated with MPD at 25 μM for 12, 24 and 48 h, respectively. (D) The relative quantity of ROS level in VECs ($^{\#}p < 0.01$ vs normal group, $^*p < 0.05$ vs control group, $^{**}p < 0.01$ vs control group, $n = 3$).

expression, but it could not depress the ROS level induced by deprivation of serum and FGF-2.²⁰ In the present study, we found that MPD more effectively inhibited VEC apoptosis at low concentrations than 3BDO. Moreover, it not only depressed the level of integrin $\beta 4$, but also suppressed the increase of ROS induced by deprivation of serum and FGF-2. The data suggested that MPD would provide much information about the relationship between integrin $\beta 4$ and ROS in regulation of VEC apoptosis, and it was a more potential inhibitor of VEC apoptosis than 3BDO.

In the past decades, considerable progress has been made in understanding how integrin $\beta 4$ regulated cell function, and most researches were focused on carcinoma cells. However, the function of this integrin in normal VECs is not well known. In our previous studies, we found that integrin $\beta 4$ was involved in VEC apoptosis and the results showed that integrin $\beta 4$ mediated VEC apoptosis through modulating the levels of ROS and p53, suggesting that integrin $\beta 4$, ROS, and p53 regulated VEC apoptosis in a cooperative manner.^{20,25,30} The data of the present study support our previous reports.

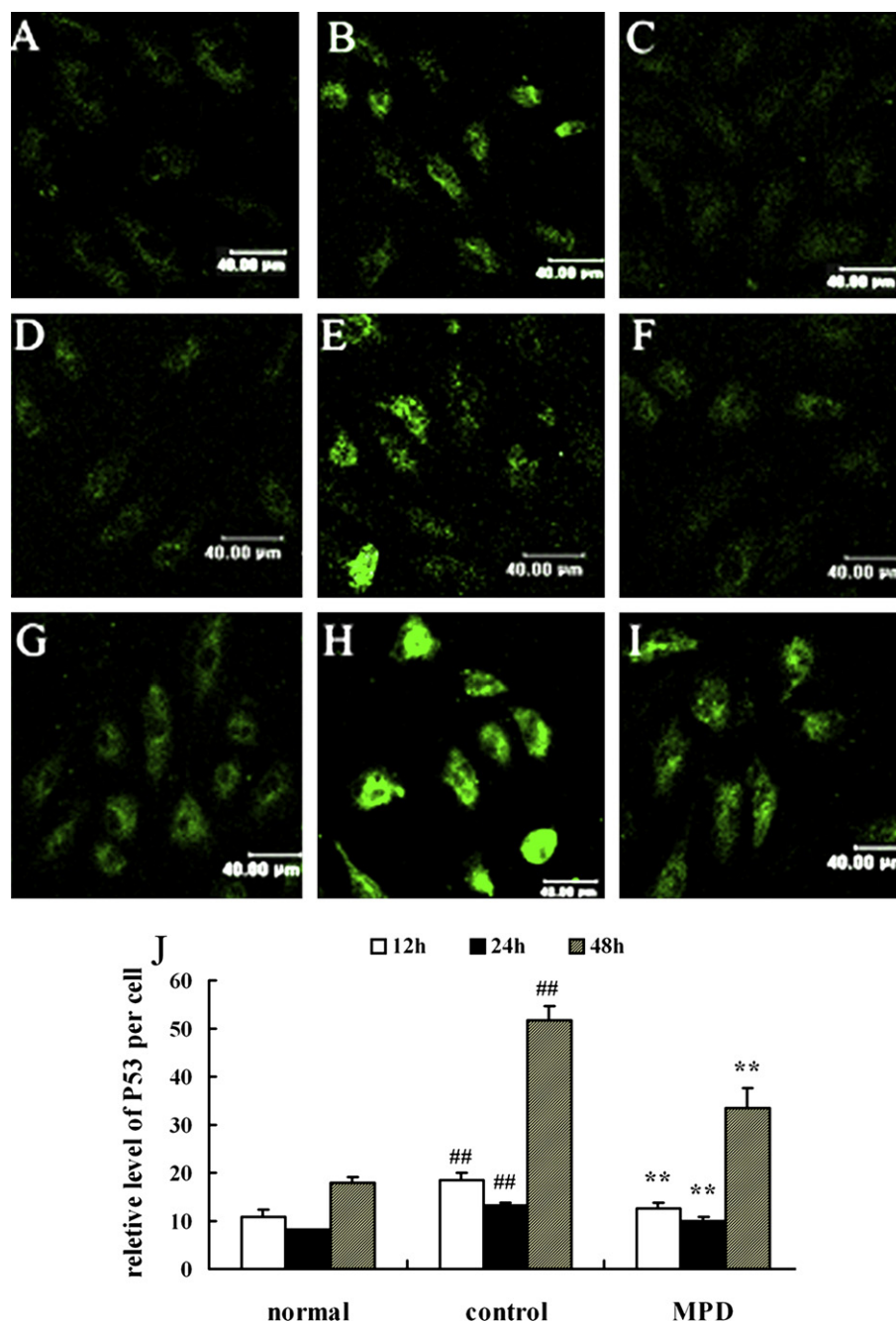


Figure 7. Effects of MPD on the level of p53 in VECs. (A–I) Fluorescent micrographs show the relative intensity of p53. (A, D and G) Normal, cells cultured in M199 medium with serum and FGF-2 for 12, 24 and 48 h, respectively. (B, E and H) Control, cells deprived of serum and FGF-2 for 12, 24 and 48 h, respectively. (C, F and I) Cells treated with MPD at 25 μM for 12, 24 and 48 h, respectively. (J) The relative quantity of p53 level in VECs (** $p < 0.01$ vs control group, ## $p < 0.01$ vs normal group, $n = 3$).

3. Conclusion

In summary, multi-substituted pyrazole derivatives were synthesized and preliminary biological evaluation in VEC apoptosis were determined. By screening, we discovered ethyl 3-(*o*-chlorophenyl)-5-methyl-1-phenyl-1*H*-pyrazole-4-carboxylate (MPD) should be a potential inhibitor of VEC apoptosis induced by deprivation of serum and FGF-2. It inhibited the apoptosis through down-regulating the levels of integrin β4, p53, and ROS. Cell-permeable MPD with anti-apoptotic effects in VECs offered us an exciting tool to study the mecha-

nism of VEC apoptosis, and MPD might be useful in the development of new strategies in vascular disease therapy.

4. Experimental

4.1. General methods

Thin-layer chromatography (TLC) was conducted on silica gel 60 F₂₅₄ plates (Merck KgaA). ¹H NMR spectra were recorded on JEOL-FX-90Q instrument, using

CDCl₃ or DMSO as solvent. Melting points were determined on an XD-4 digital micro melting point apparatus. IR spectra were recorded with an IR spectrophotometer Avtar 370 FT-IR (Thermo Nicolet). MS spectra were recorded on a Trace DSQ mass spectrophotometer (Thermo Finnigan).

4.2. General procedure for the synthesis of *Z*-ethyl 2-(hydroxy(aryl)methylene)-3-oxobutanoate **3a–3d** (for a typical **3a**)

To the mixture of ethyl acetoacetate (13 g, 0.1 mol) and petroleum ether (17 mL) was added 33% (w/w) of solution of sodium hydroxide (5 mL), and the mixture was stirred for 30 min at 0 °C. Then, 2-chlorobenzoyl chloride (13.6 mL, 0.105 mol) and 33% (w/w) of solution of sodium hydroxide (18 mL) were added dropwise from two funnel, respectively. After stirring for 1 h at 0 °C, the mixture was heated to 35 °C and stirred for 1 h. Then cooled overnight, precipitate was filtered, washed with water and petroleum ether, dried, to afford *Z*-ethyl 2-(hydroxy(*o*-chlorophenyl)methylene)-3-oxobutanoate **3a** 16.4 g (yield 61%).

4.2.1. *Z*-Ethyl 2-(hydroxy(*o*-chlorophenyl)methylene)-3-oxobutanoate **3a.** White solid, mp 229–232 °C; IR (KBr) *v*: 2980, 1681, 1620, 1600, 1409, 1390, 1342, 1282, 1086, 766 cm⁻¹; ¹H NMR (DMSO) δ : 7.01–7.21 (m, 4H, ArH), 3.48 (q, *J* = 7.2 Hz, 2H, CH₂CH₃), 2.07 (s, 3H, CH₃), 0.54 (t, *J* = 7.2 Hz, 3H, CH₂CH₃). Anal. Calcd for C₁₃H₁₃ClO₄: C, 58.11; H, 4.88. Found: C, 58.14; H, 4.85.

4.2.2. *Z*-Ethyl 2-(hydroxy(*o*-nitrophenyl)methylene)-3-oxobutanoate **3b.** Pale yellow solid, yield 64%, mp 123–124 °C; IR (KBr) *v*: 2987, 1678, 1649, 1600, 1567, 1526, 1389, 1343, 1088, 863, 706 cm⁻¹; ¹H NMR (DMSO) δ : 7.88–7.97 (m, 1H, ArH), 7.39–7.58 (m, 2H, ArH), 7.13–7.20 (m, 1H, ArH), 3.62 (q, *J* = 7.3 Hz, 2H, CH₂CH₃), 2.17 (s, 3H, CH₃), 0.64 (t, *J* = 7.3 Hz, 3H, CH₂CH₃). Anal. Calcd for C₁₃H₁₃NO₆: C, 55.91; H, 4.69; N, 5.02. Found: C, 55.89; H, 4.72; N, 5.04.

4.2.3. *Z*-Ethyl 2-(hydroxy(*p*-nitrophenyl)methylene)-3-oxobutanoate **3c.** Pale yellow solid, yield 95%, mp 128–131 °C; IR (KBr) *v*: 3537, 3394, 2986, 1658, 1646, 1583, 1520, 1383, 1346, 1078, 981, 840, 712 cm⁻¹; ¹H NMR (DMSO) δ : 8.08 (d, *J* = 8.5 Hz, 2H, ArH), 7.40 (d, *J* = 8.5 Hz, 2H, ArH), 3.53 (q, *J* = 7.3 Hz, 2H, CH₂CH₃), 2.07 (s, 3H, CH₃), 0.56 (t, *J* = 7.3 Hz, 3H, CH₂CH₃). Anal. Calcd for C₁₃H₁₃NO₆: C, 55.91; H, 4.69; N, 5.02. Found: C, 55.95; H, 4.75; N, 4.98.

4.2.4. *Z*-Ethyl 2-(hydroxy(*p*-tolyl)methylene)-3-oxobutanoate **3d.** White solid, yield 85%, mp 221–223 °C; IR (KBr) *v*: 2977, 1696, 1657, 1598, 1410, 1234, 1067, 903, 782, 773 cm⁻¹; ¹H NMR (DMSO) δ : 7.23 (d, *J* = 8.3 Hz, 2H, ArH), 7.00 (d, *J* = 8.3 Hz, 2H, ArH), 3.50 (q, *J* = 7.2 Hz, 2H, CH₂CH₃), 2.23 (s, 3H, CH₃ in CH₃C₆H₄), 2.01 (s, 3H, C=OCH₃), 0.50 (t, *J* = 7.2 Hz, 3H, CH₂CH₃). Anal. Calcd for C₁₄H₁₆O₄: C, 67.73; H, 6.50. Found: C, 67.69; H, 6.52.

4.3. Synthesis of multi-substituted pyrazole derivatives **4** (**4a** for a typical procedure)

4.3.1. Ethyl 3-(*o*-chlorophenyl)-5-methyl-1*H*-pyrazole-4-carboxylate **4a.** To a stirred solution of the *Z*-ethyl 2-(hydroxy(*o*-chlorophenyl)methylene)-3-oxobutanoate (5.37 g, 0.02 mol) in ethanol (250 mL), hydrazine (0.06 mol, 80%) was added dropwise at room temperature. The reaction mixture was stirred at refluxing for 19 h. Then the mixture was concentrated under reduced pressure, and the residue was dissolved in ethyl acetate, washed with water, organic phase was dried over MgSO₄. After concentration, the residue was chromatographed on silica gel by elution of petroleum and ethyl acetate (1:1 V/V) to give **4a** (4.3 g, yield 79%); IR (KBr) *v*: 3190, 2981, 1708, 1492, 1294, 1184, 1104, 989, 763 cm⁻¹; ¹H NMR (CDCl₃) δ : 11.60 (s, 1H, NH), 7.22–7.35 (m, 4H, ArH), 4.01 (q, *J* = 7.3 Hz, 2H, CH₂CH₃), 2.01 (s, 3H, CH₃), 0.96 (t, *J* = 7.3 Hz, 3H, CH₂CH₃); MS *m/z* (%): 229 (M⁺–Cl, 86), 201 (100), 200 (18), 127 (24), 126 (16), 75 (16). Anal. Calcd for C₁₃H₁₃ClN₂O₂: C, 58.99; H, 4.95; N, 10.58. Found: C, 58.96; H, 4.98; N, 10.60.

4.3.2. Ethyl 5-methyl-3-(*o*-nitrophenyl)-1*H*-pyrazole-4-carboxylate **4b.** Pale gray solid, yield 71%, mp 137–141 °C; IR (KBr) *v*: 3194, 1685, 1606, 1527, 1350, 750 cm⁻¹; ¹H NMR (CDCl₃) δ : 10.70 (s, 1H, NH), 7.46–8.05 (m, 4H, ArH), 3.99 (q, *J* = 7.3 Hz, 2H, CH₂CH₃), 2.20 (s, 3H, CH₃), 1.00 (t, *J* = 7.3 Hz, 3H, CH₂CH₃); MS *m/z* (%): 230 (M⁺–OEt, 20), 229 (62), 201 (100), 184 (16), 129 (12), 103 (20), 76 (16), 42 (18). Anal. Calcd for C₁₃H₁₃N₃O₄: C, 56.72; H, 4.76; N, 15.27. Found: C, 56.69; H, 4.79; N, 15.30.

4.3.3. Ethyl 5-methyl-3-(*p*-nitrophenyl)-1*H*-pyrazole-4-carboxylate **4c.** Yellow solid, yield 42%, mp 156–157 °C; IR (KBr) *v*: 3343, 3221, 1699, 1677, 1518, 1351, 854, 788 cm⁻¹; ¹H NMR (CDCl₃) δ : 10.36 (s, 1H, N–H), 8.25 (d, *J* = 8.2 Hz, 2H, ArH), 7.83 (d, *J* = 8.2 Hz, 2H, ArH), 4.25 (q, *J* = 7.0 Hz, 2H, CH₂CH₃), 2.56 (s, 3H, CH₃), 1.26 (t, *J* = 7.0 Hz, 3H, CH₂CH₃); MS *m/z* (%): 275 (M⁺, 50), 247 (30), 230 (100), 229 (24), 200 (10), 184 (45), 128 (20), 115 (13), 77 (14), 42 (9). Anal. Calcd for C₁₃H₁₃N₃O₄: C, 56.72; H, 4.76; N, 15.27. Found: C, 56.75; H, 4.78; N, 15.25.

4.3.4. Ethyl 3-(*o*-chlorophenyl)-5-methyl-1-phenyl-1*H*-pyrazole-4-carboxylate **4d.** White solid, yield 76%, mp 153–157 °C; IR (KBr) *v*: 3064, 2980, 1709, 1597, 1504, 1244, 1105, 758, 692 cm⁻¹; ¹H NMR (CDCl₃) δ : 7.13–7.30 (m, 9H, ArH), 3.95 (q, *J* = 7.3 Hz, 2H, CH₂CH₃), 2.54 (s, 3H, CH₃), 0.97 (t, *J* = 7.3 Hz, 3H, CH₂CH₃); MS *m/z* (%): 340 (M⁺, 20), 339 (76), 311 (100), 277 (9), 190 (6), 126 (5), 77 (38), 51 (9). Anal. Calcd for C₁₉H₁₇ClN₂O₂: C, 66.96; H, 5.03; N, 8.22. Found: C, 66.98; H, 5.00; N, 8.20.

4.3.5. 3-(*o*-Nitrophenyl)-1-phenyl-1*H*-pyrazol-5-ol **4e.** Pale yellow solid, yield 69%, mp 139–140 °C; IR (KBr) *v*: 3384, 3339, 1675, 1539, 1497, 1347, 859, 767 cm⁻¹; ¹H NMR (DMSO) δ : 10.36 (s, 1H, OH), 7.21–8.09 (m, 5H, ArH), 6.59–7.12 (m, 5H, ArH and pyrazole); MS

m/z (%): 281 (M^+ , 8), 223 (12), 196 (15), 195 (100), 167 (83), 166 (45), 139 (20), 91 (18), 77 (38), 43 (32). Anal. Calcd for $C_{15}H_{11}N_3O_3$: C, 64.05; H, 3.94; N, 14.94. Found: C, 64.02; H, 3.97; N, 14.90.

4.3.6. 3-*p*-Tolyl-1*H*-pyrazol-5-ol 4f. White solid, yield 85%, mp 223–226 °C; IR (KBr) *v*: 3123, 2585, 1627, 1605, 1513, 930, 826, 775 cm^{-1} ; 1H NMR (DMSO) δ : 10.60 (s, 2H, NH and OH), 7.50 (d, $J = 8.2$ Hz, 2H, ArH), 7.14 (d, $J = 8.2$ Hz, 2H, ArH), 5.78 (s, 1H), 2.25 (s, 3H, CH_3); MS *m/z* (%): 174 (M^+ , 100), 145 (5), 131 (10), 117 (45), 115 (25), 91 (15), 73 (8), 58 (15), 43 (33). Anal. Calcd for $C_{10}H_{10}N_2O$: C, 68.95; H, 5.79; N, 16.08. Found: C, 68.91; H, 5.81; N, 16.11.

4.4. Biological assay

4.4.1. Cell culture. Human umbilical vein endothelial cells (HUVECs) were obtained as described previously.³³ The cells were cultured on gelatin-coated plastic dishes with M199 medium (Gibco, USA) with 20% fetal bovine serum (FBS, Hyclone Lab Inc., USA) and 70 ng/mL FGF-2, at 37 °C in 5% CO_2 and 95% air (normal group). All experiments were performed on cells from 10 to 20 passages.

4.4.2. Exposure of VEC to compounds 4. When the cultures of VEC reached sub-confluence, the culture medium was replaced with basal M199 culture medium (without FGF-2 and FBS) after once wash with the same medium. Then the cells were treated in three ways. (a) Cells were cultured in M199 medium with serum and FGF-2 (normal group). (b) Cells were cultured in basal M199 medium (control group). (c) Cells were cultured in basal M199 medium with compounds 4 at 25–100 μM , particularly with compound 4d at 5–100 μM (MPD group). Compounds 4 were dissolved in dimethyl sulfoxide (DMSO) and applied to cells such that DMSO at the final concentration did not affect the viability of the cells. The morphological changes of cells were observed with phase contrast microscope (Nikon, Japan) at 24 and 48 h, respectively.

4.4.3. Cell growth assay. When the cells cultured on 96-well cell culture plate reached sub-confluence (the cells did not contact with each other), the cells were washed once with M199 medium and then, were cultured in the medium without serum and FGF-2 (control group). The cells were treated with compound 4 at 25–100 μM , particularly with compound 4d, at 5, 10, 20, 25, 50, and 100 μM , respectively. At 24 and 48 h, cell viability was determined by 3-[4,5-dimethylthiazol-2-yl]-2,5-diphenyl-tetrazolium (MTT) assay following the procedure described by Price and McMillan.³⁴

4.4.4. Nuclear fragmentation assay. The cells treated with MPD for 24 h were stained with acridine orange (AO) for 5 min, the nuclear fragmentation was observed under a laser scanning confocal microscope (Leica, Germany).

4.4.5. Terminal deoxynucleotidyl transferase-mediated dUTP nick-end labeling (TUNEL) assay. The TdT-med-

iated dUTP nick-end labeling technique was used to detect in situ nuclear DNA fragmentation and count apoptosis ratio.³⁵ The cells treated as above-mentioned three ways for 24 h, then DNA fragmentation was detected by the DeadEnd™ Fluorometric TUNEL System (Promega, USA) according to the manufacturer's protocol. Samples were evaluated under the laser scanning confocal microscope (Leica, Germany). The apoptosis rate was quantified according to the TUNEL-positive rate.

4.4.6. Immunofluorescence. Immunofluorescence was performed as the method of Zhao et al.³⁶ After adding the primary (rabbit anti-human p53, integrin $\beta 4$) and second antibodies (FITC-IgG) (Santa Cruz Biotechnology), samples were evaluated with laser scanning confocal microscopy (Leica, Germany). The immunofluorescence techniques allow semiquantitative evaluation of protein expression.³⁷

4.4.7. ROS assay. The levels of intracellular ROS were detected in cells treated with or without MPD using a fluorescent probe, 2',7'-dichlorodihydrofluorescein (DCHF, Sigma, USA), which can be oxidized into fluorescent 2',7'-dichlorofluorescein (DCF) by intracellular ROS. This assay is a reliable method for measuring the intracellular ROS.³⁸ The fluorescence was monitored with laser scanning confocal microscopy (Leica, Germany). The amount of ROS was quantified as the relative fluorescence intensity of DCF per cell in the scanned area.

4.4.8. Statistics analysis. The results are expressed as means \pm SE. Statistical analysis was done by *t* test, and differences at $p < 0.05$ were considered statistically significant.

Acknowledgments

This work was financially supported by the National 973 Research Project (No. 2006CB503803) and by Natural Science Foundation of Shandong Province (Y2005B12 and Z2006D02).

References and notes

1. Ross, R. *Adv. Nephrol. Necker. Hosp.* **1990**, *19*, 79.
2. Dimmeler, S.; Hermann, C.; Zeiher, A. M. *Eur. Cytokine Netw.* **1998**, *9*, 697.
3. Huber, J.; Vales, A.; Mitulovic, G., et al. *Arterioscler. Thromb. Vasc. Biol.* **2002**, *22*, 101.
4. Cole, A. L.; Subbanagounder, G.; Mukhopadhyay, S.; Berliner, J. A.; Vora, D. K. *Arterioscler. Thromb. Vasc. Biol.* **2003**, *23*, 1384.
5. Bombeli, T.; Karsan, A.; Tait, J. F.; Harlan, J. M. *Blood* **1997**, *89*, 2429.
6. Yeh, J.-R. J.; Crews, C. M. *Dev. Cell* **2003**, *5*, 11.
7. Stockwell, B. R. *Trends Biotechnol.* **2000**, *18*, 449.
8. Schreiber, S. L. *Bioorg. Med. Chem.* **1998**, *6*, 1127.
9. Khersonsky, S. M.; Chang, Y.-T. *Chembiochem* **2004**, *5*, 903.
10. Burke, M. D.; Schreiber, S. L. *Angew. Chem. Int. Ed.* **2004**, *43*, 46.

11. Hashimoto, H.; Imamura, K.; Haruta, J.-I.; Wakitani, K. *J. Med. Chem.* **2002**, *45*, 1511.
12. Habeeb, A. G.; Rao, P. N. P.; Knaus, E. E. *J. Med. Chem.* **2001**, *44*, 3039.
13. Ranatunge, R. R.; Earl, R. A.; Garvey, D. S.; Janero, D. R.; Letts, L. G.; Martino, A. M.; Murty, M. G.; Richardson, S. K.; Schwalb, D. J.; Young, D. V.; Zemtseva, I. S. *Bioorg. Med. Chem. Lett.* **2004**, *14*, 6049.
14. Singh, S. K.; Saibaba, V.; Rao, K. S.; Reddy, P. G.; Daga, P. R.; Rajjak, S. A.; Misra, P.; Rao, Y. K. *Eur. J. Med. Chem.* **2005**, *40*, 977.
15. Elzein, E.; Kalla, R.; Li, X.; Perry, T.; Parkhill, E.; Palle, V.; Varkhedkar, V.; Gimbel, A.; Zeng, D.; Lustig, D.; Leung, D.; Zablocki, J. *Bioorg. Med. Chem. Lett.* **2006**, *16*, 302.
16. Xia, Y.; Dong, Z.-W.; Zhao, B.-X.; Ge, X.; Meng, N.; Shin, D. S.; Miao, J. Y. *Bioorg. Med. Chem.* **2007**, *15*, 6893.
17. Wei, F.; Zhao, B.-X.; Huang, B.; Zhang, L.; Sun, C.-H.; Dong, W.-L.; Shin, D.-S.; Miao, J.-Y. *Bioorg. Med. Chem. Lett.* **2006**, *16*, 6342.
18. Ding, X.-L.; Meng, N.; Xia, Y.; Wang, L.-J.; Zhang, X.-F.; Zhao, B.-X.; Miao, J.-Y. *Chin. J. Org. Chem.* **2007**, *27*, 1542.
19. Xie, Y.-S.; Pan, X.-H.; Zhao, B.-X.; Liu, J.-T.; Shin, D.-S.; Zhang, J.-H.; Zheng, L.-W.; Zhao, J.; Miao, J.-Y. *J. Organomet. Chem.* **2008**. doi:10.1016/j.jorganchem.2008.01.043.
20. Wang, W.-W.; Liu, X.; Zhao, J.; Zhao, B.-X.; Zhang, S.-L.; Miao, J.-Y. *Bioorg. Med. Chem. Lett.* **2007**, *17*, 482.
21. Zhao, J.; Miao, J.-Y.; Zhao, B.-X.; Zhang, S.-L. *FEBS Lett.* **2005**, *579*, 5809.
22. Zhao, J.; Miao, J.-Y.; Zhao, B.-X.; Zhang, S.-L. *Int. J. Biochem. Cell Biol.* **2006**, *38*, 1603.
23. Ginsbergil, H. F.; Lederman, I.; Papa, D. *J. Am. Chem. Soc.* **1953**, *75*, 4587.
24. Miao, J.-Y.; Zhao, B.-X.; Li, H.-H.; Zhang, S.-L.; Du, C.-Q. *Acta Pharmacol. Sin.* **2002**, *23*, 323.
25. Miao, J. Y.; Araki, S.; Kaji, K.; Hayashi, H. *Biochem. Biophys. Res. Commun.* **1997**, *233*, 182.
26. Laferriere, J.; Houle, F.; Huot, J. *Clin. Exp. Metastasis* **2004**, *21*, 257.
27. Giancotti, F. G. *Trends Pharmacol. Sci.* **2007**, *28*, 506.
28. Dowling, J.; Yu, Q. C.; Fuchs, E. *J. Cell Biol.* **1996**, *134*, 559.
29. Zhao, Q.-T.; Wang, N.; Jia, R.; Zhan, S.-L.; Miao, J.-Y. *Vascul. Pharmacol.* **2004**, *41*, 1.
30. Zhao, J.; Miao, J.-Y.; Zhao, B.-X.; Zhang, S.-L. *FEBS Lett.* **2005**, *579*, 5809.
31. Liu, X.; Yin, D.-L.; Zhang, Y.; Zhao, J.; Zhang, S.-L.; Miao, J.-Y. *FEBS Lett.* **2007**, *581*, 5337.
32. Zhao, J.; Zhao, B.-X.; Du, A.-Y.; Zhao, Q.-T.; Miao, J.-Y. *Endothelium* **2004**, *11*, 267.
33. Jaffe, E. A.; Nachman, R. L.; Becker, C. G. *J. Clin. Invest.* **1973**, *52*, 2745.
34. Price, P.; McMillan, T. J. *Cancer Res.* **1990**, *50*, 1392.
35. Zhang, Z.; Dickerson, I. M.; Russo, A. F. *Endocrinology* **2006**, *147*, 1932.
36. Zhao, Q.; Araki, S.; Zhang, S.; Miao, J. *Toxicol.* **2004**, *44*, 161.
37. Babcock, G. F. *Methods Enzymol.* **1999**, *307*, 319.
38. Suematsu, N.; Tsutsui, H.; Wen, J.; Kang, D.; Ikeuchi, M.; Ide, T.; Hayashidani, S.; Shiomi, T.; Kubota, T.; Hamasaki, N.; Takeshita, A. *Circulation* **2003**, *107*, 1418.